



Intrinsic Transport Properties and Performance Limits of Organic Field- Effect Transistors

L. Torsi; A. Dodabalapur; L. J. Rothberg; A. W. P. Fung; H. E. Katz

Science, New Series, Vol. 272, No. 5267. (Jun. 7, 1996), pp. 1462-1464.

Stable URL:

<http://links.jstor.org/sici?sici=0036-8075%2819960607%293%3A272%3A5267%3C1462%3AITPAPL%3E2.0.CO%3B2-W>

Science is currently published by American Association for the Advancement of Science.

Your use of the JSTOR archive indicates your acceptance of JSTOR's Terms and Conditions of Use, available at <http://www.jstor.org/about/terms.html>. JSTOR's Terms and Conditions of Use provides, in part, that unless you have obtained prior permission, you may not download an entire issue of a journal or multiple copies of articles, and you may use content in the JSTOR archive only for your personal, non-commercial use.

Please contact the publisher regarding any further use of this work. Publisher contact information may be obtained at <http://www.jstor.org/journals/aaas.html>.

Each copy of any part of a JSTOR transmission must contain the same copyright notice that appears on the screen or printed page of such transmission.

The JSTOR Archive is a trusted digital repository providing for long-term preservation and access to leading academic journals and scholarly literature from around the world. The Archive is supported by libraries, scholarly societies, publishers, and foundations. It is an initiative of JSTOR, a not-for-profit organization with a mission to help the scholarly community take advantage of advances in technology. For more information regarding JSTOR, please contact support@jstor.org.

Intrinsic Transport Properties and Performance Limits of Organic Field-Effect Transistors

L. Torsi,*† A. Dodabalapur,* L. J. Rothberg, A. W. P. Fung, H. E. Katz

The field-effect mobility in thin-film transistors based on α -sexithiophene (α -6T) and related materials displays a temperature dependence that is remarkably nonmonotonic. Above a transition temperature T_T (specific to a given material) the transport is thermally activated, whereas below T_T there is a very steep enhancement of the mobility. In the activated regime, the results are well described by the theoretical predictions for small polaron motion made by Holstein in 1959. An analysis of the transistor characteristics shows that the hopping transport in these devices is intrinsic. Performance limits for devices based on α -6T and related materials were established; these limits point to the strong possibility that better molecular materials for transistor applications may be designed from first principles.

The prospect of field-effect transistors (FETs) made from easily processable thin organic films is generating considerable interest. Much of this interest springs from the possibility of using such transistors in such applications as smart cards and flexible displays. In some of these applications, charge-carrier mobilities greater than $10^{-2} \text{ cm}^2 \text{ V}^{-1} \text{ s}^{-1}$ are required. Although a number of different organic-polymeric materials have been used as thin-film transistor (TFT) active materials, oligothiophenes such as α -6T and oligothiophene derivatives such as α - ω dihexyl sexithiophene (H-6T) have emerged as particularly promising molecular solids (1–3). These materials form polycrystalline films in which the long axis of the molecules stands almost perpendicular to the substrate (4), and the transport direction in the TFTs is perpendicular to the molecular chains (see inset of Fig. 1A). A deeper understanding of the fundamentals of carrier transport will enable us to assess performance limits and eventually will point to new materials that might have superior transport properties.

We studied the field-effect mobility (μ_{FET}) of α -6T and H-6T at temperatures T from 4 to 350 K, which extends the range of such measurements to below 77 K (5). The FET, aside from its potential utility, is a powerful means to study fundamental transport phenomena in thin-film organic materials (6), particularly oriented molecular crystals. The measurement of $\mu_{\text{FET}}(T)$ shows that it decreases with decreasing T up to a critical point, T_T (typically ~ 50 K), and then abruptly increases by several orders of magnitude when T is lowered beyond T_T . We attribute this unusual nonmonotonic be-

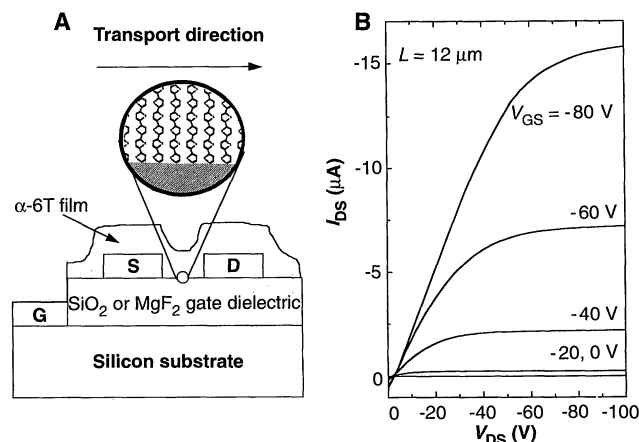
havior to a transition from localized to delocalized charge carrier motion as predicted by Holstein (7, 8). This theory on the motion of small polarons in a molecular crystal has been used by many researchers to partially explain the T dependence of charge drift mobilities in a variety of systems such as muonium in KCl (9). Our application of Holstein's theory to oligothiophene molecular crystals has made possible the understanding of transport phenomena in materials such as α -6T with a degree of depth and accuracy that has not been possible so far and offers a way to calculate mobilities directly from material parameters. It may therefore afford a way to select better materials for TFT applications.

The schematic transistor structure is shown in Fig. 1A. The drain-source current (I_{DS}) as a function of the drain-source voltage (V_{DS}) is shown in Fig. 1B for different gate voltages (V_{GS}). These I - V characteris-

tics were measured at several points between 4 and 350 K, and analytical modeling, described in (10), allows us to extract the measured μ_{FET} . Typically the μ_{FET} values are about $0.02 \text{ cm}^2 \text{ V}^{-1} \text{ s}^{-1}$ for the α -6T TFT (2) and $0.05 \text{ cm}^2 \text{ V}^{-1} \text{ s}^{-1}$ for the H-6T TFT (11) at room temperature. The TFTs were fabricated as reported in (2).

In Fig. 2, the μ_{FET} values of α -6T TFTs are plotted as a function of T . The mobility falls exponentially with decreasing T until $T_T \sim 45$ K; below T_T , it abruptly increases by more than two orders of magnitude and then remains approximately constant. Such behavior was observed in many sets of samples, both in α -6T and H-6T thin films and with a variety of TFT geometries. At low T , μ_{FET} and the critical carrier density n_T (proportional to V_T , the TFT threshold voltage) were the only sample-dependent features. The key role played by n_T is illustrated in Fig. 3A, where I_{DS} is plotted as a function of T for two values of V_{GS} . At $V_{\text{GS}} = 0$, the only charges in the channel of the device are those due to adventitious dopants present in the material (typically 10^{16} to 10^{17} cm^{-3} or 5×10^{10} to $5 \times 10^{11} \text{ cm}^{-2}$ at room temperature for α -6T used in these measurements) and I_{DS} remains approximately constant with temperature. When a negative V_{GS} is applied (for example -80 V), the carrier density in the channel is greatly enhanced and I_{DS} rises sharply as T is lowered below ~ 45 K. In Fig. 3B, the square root of I_{DS} [proportional to μ_{FET} (12)] along with the total sheet carrier density, n , at 4 K is plotted as a function of V_{GS} . The points are along a straight line, and the intercept yields the n_T necessary to observe the mobility increase at low T . The value of n_T was found to be sample-dependent and was smaller for samples with a higher room-temperature μ_{FET} . The fact that the exper-

Fig. 1. (A) TFT structure: a conductive Si substrate, with an Au contact, functions as a gate (G), and either SiO_2 (300 nm) or MgF_2 (100 nm) is the gate dielectric. Source (S) and drain (D) Au pads (width = $250 \mu\text{m}$) are photolithographically defined on top of the dielectric. The channel length L (12 or $25 \mu\text{m}$) is the separation between the S and D contacts. The thin (50 nm) organic film (α -6T or α , ω H-6T) is thermally evaporated (base pressure 10^{-7} to 10^{-6} torr) over the gate dielectric. The inset shows that α -6T molecules are oriented almost perpendicular to the substrate and the transport direction is transverse to the chains. **(B)** Source-drain current versus voltage characteristics of α -6T TFT with $L = 12 \mu\text{m}$ at different gate voltages. These I - V characteristics are typical of a p -channel FET and show distinct linear and saturated regions.



Bell Laboratories, Lucent Technologies, 600 Mountain Avenue, Murray Hill, NJ 07974, USA.

*To whom correspondence should be addressed.

†Present address: Department of Chemistry, University of Bari, Bari I-70126, Italy.

imental points in Fig. 3B lie along a straight line constitutes evidence that the transport is intrinsic, as discussed below.

Another important characteristic of the T dependence of μ_{FET} is that, at T_T , μ_{FET} reaches a minimum (Fig. 2A and Fig. 3A). The T_T value is independent of V_{GS} and transistor geometry (such as channel length L), but T_T does depend on the material: The H-6T TFTs had a $T_T \sim 60$ K; in contrast, α -6T had a TFT of 45 K. As we discuss below, in the context of Holstein's picture, T_T is related to the Debye temperature Θ_D , which is material-specific.

We can interpret the striking variation of μ_{FET} with T shown in Fig. 2 within the framework of Holstein's theory on small polaron motion (7). The high- T mobility ($T > T_T$) agrees quantitatively with the theory, which states that highly localized small polarons (that is, polarons localized to a single α -6T chain) move by hopping from one molecule to the next. The transition temperature is given by $T_T \sim 0.4 \Theta_D$ (7) and is related to the vibrational energy, $\hbar\omega_0$ (where $\hbar = h/2\pi$ and h is Planck's constant), of the phonon involved in the hopping process by $\hbar\omega_0 \sim k_B \Theta_D$, where k_B is the Boltzmann constant. The phonon energy $\hbar\omega_0$ is therefore 10 meV, which is consistent with this being an intermolecular phonon (13) as would be expected to assist transverse the hopping of small polarons in conjugated systems (14). An order of magnitude estimate for the maximum electronic bandwidth is $J \sim \hbar\omega_0$ (7), a value consistent with the idea that J is the electronic overlap of π -orbitals. When the above values for J and ω_0 and the measured intermolecular distance 3.8 Å were used (15), the expression for the high- T mobility [equation 97 in (7)] yields a value of 10 for γ , a dimensionless parameter, that describes the strength of the electron-phonon interaction in the material. This value of γ is indicative of a strong electron-phonon interaction.

As a result, the polaron binding energy E_B , which is $\sim \gamma \hbar\omega_0$ according to Holstein, is estimated to be ~ 100 meV. This value is in reasonably good agreement with the optically measured E_B (16), because E_B is supposed to be several times larger than γ (17). It also satisfies the small polaron condition $J < E_B/2$ (7). The satisfaction of the above inequality, together with the large value of γ resulting from the fit, clearly show that small polarons are the mobile charges in oligothiophene devices. If we use the elicited values for J , γ , and ω_0 in the low- T mobility expression [equation 101 in (7)], the agreement (before the leveling off of the mobility occurs) is excellent, as can be seen in Fig. 2. The observation of such an abrupt increase in μ_{FET} also establishes the striking similarities between this system and the predictions

of Holstein for small-polaron motion.

There are various theoretical difficulties in using Holstein's theory for temperatures below T_T , the chief of which is Holstein's statement that band transport occurs for $T < T_T$. This does not appear to be the case in our samples, because μ_{FET} ($\sim 10^{-2} \text{ cm}^2 \text{ V}^{-1} \text{ s}^{-1}$) is below the required value on the basis of Mott's minimum metallic conductivity considerations (8). The de Broglie length (18) in this regime is also much less than the mean free path. We conjecture that the transition, although not necessarily from hopping to band transport as predicted by Holstein, is rather between the motion of highly localized small polarons and more delocalized lighter polarons. The complete delocalization of those charges is prevented because of scattering by defects that are present in the material and cause the mobility to level off at low T . We expect much higher mobilities at $T < T_T$ in perfect α -6T single crystals, a hypothesis supported by the sample dependence of μ_{FET} at low T (19). Because of the very narrow width of the polaron band, which Holstein calculates to be $W_p \sim 2Je^{-\gamma}$ (10^{-6} to 10^{-7} eV), the Bloch band-like regime could be difficult to access in real crystals.

Clearly, there is room for further theoretical development, particularly at low T , and we are hopeful that such data from organic TFTs will be useful to theorists studying small-polaron motion (20). The sharp increase in μ_{FET} below T_T could, in principle, be attributed to the occurrence of a structural phase transition. However, the very low probability of such transitions at these low temperatures (of order one-tenth the glass

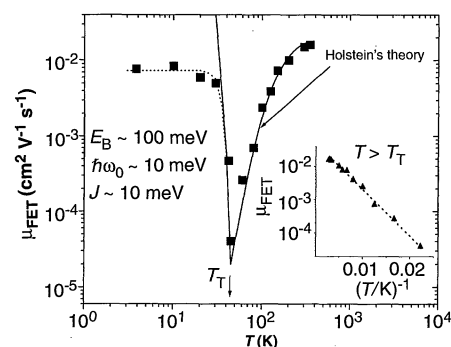


Fig. 2. Measured μ_{FET} values of α -6T TFTs (squares) versus T . The total density of induced charges is $n = 4.8 \times 10^{12} \text{ cm}^{-2}$ as determined from $n = C_i V_{\text{GS}}/q$, where V_{GS} is the applied gate voltage, q is the elemental charge, and C_i is the gate dielectric capacitance per unit area. However, the mobility is independent of the charge density beyond a threshold value to be defined in Fig. 3. The transition temperature (see text) is T_T , and the continuous line is Holstein's theoretical prediction (7). The value of the mobility for $T < T_T$ (dotted line) is an adjustable parameter. The inset shows μ_{FET} (triangles) versus T^{-1} for $T > T_T$.

transition temperature) (21) leads us to favor the carrier delocalization picture described above. Finally, we should note that earlier $\mu(T)$ measurements of high-quality molecular single crystals such as naphthalene (22) have been described in terms of a standard band model rather than in the framework of Holstein's theory, probably because of the weak electron-phonon interaction occurring in this class of materials.

The excellent agreement of our data with Holstein's model in the high- T regime allows us to address the intrinsic nature (that is, not dominated by grain boundary effects) of the transport mechanism that occurs in oligothiophene FETs. We have shown that at high temperatures the transport mechanism is small-polaron hopping from one molecule to its nearest neighbor. This statement is corroborated by two other

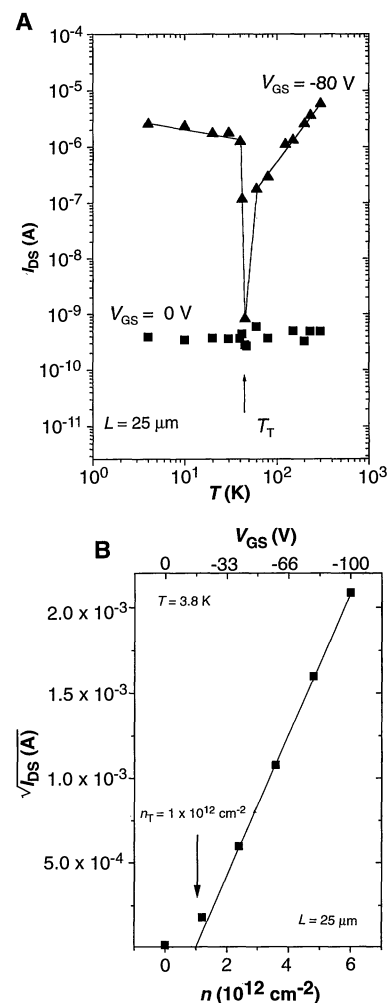


Fig. 3. (A) Plot of I_{DS} for α -6T TFTs ($L = 25 \mu\text{m}$) measured in the saturated region ($V_{\text{DS}} = -100 \text{ V}$) versus T for $V_{\text{GS}} = 0 \text{ V}$ (squares) and $V_{\text{GS}} = -80 \text{ V}$ (triangles). (B) Plot of $(I_{\text{DS}})^{1/2}$ versus the total induced charge density, n , at $T = 3.8 \text{ K}$. The value $n_T \sim 1 \times 10^{12} \text{ cm}^{-2}$ is the extracted density of charges (corresponding to the threshold gate voltage, V_T), beyond which the transistor turns on.

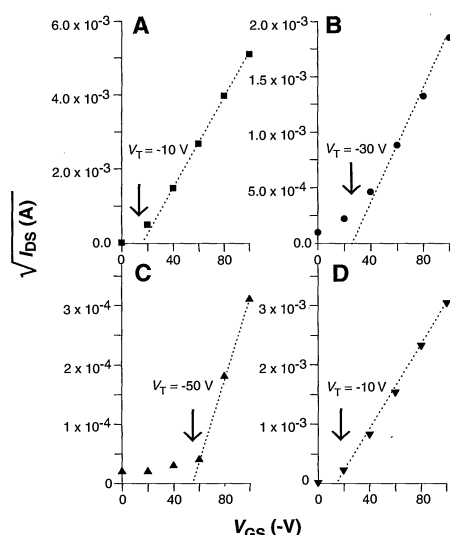


Fig. 4. Plots of $(I_{DS})^{1/2}$ versus V_{GS} for an α -6T TFT ($L = 12 \mu\text{m}$, $V_{DS} = -100 \text{ V}$) at different temperatures: (A) $T = 300 \text{ K}$; (B) $T = 100 \text{ K}$; (C) $T = 45 \text{ K}$; and (D) $T = 3.8 \text{ K}$. The intercepts of the dotted straight lines with the V_{GS} axis give the device threshold voltage (V_T), and the slopes are proportional to μ_{FET} .

independent sets of experimental evidence that show that grain boundaries do not act as the mobility-limiting mechanisms (for $n > n_T$). In (23) we showed that the room-temperature mobility in α -6T TFTs does not improve when the crystalline grains are enlarged by an order of magnitude and the grain boundaries greatly decrease in extent.

The second piece of evidence, which also indicates that grain boundaries do not dominate transport, can be obtained from the data of Fig. 4, A through D, which indicate that for $n > n_T$, the square root of I_{DS} at different temperatures increases linearly with V_{GS} (proportional to n). Particularly interesting is the $T = 3.8 \text{ K}$ case (Fig. 4D). The constant mobility in the "delocalized" regime, which occurs only within each crystallite, implies that the grain boundaries are not the mobility-limiting mechanisms. Trap filling neutralizes the effect of traps on the transport above T_T , so that intrinsic activated hopping behavior between α -6T molecules can be observed. In fact, there is always a linear relation between induced carrier density and V_{GS} beyond the threshold voltage. The surface states at the gate dielectric-active material interface also do not play a substantial role; similar behavior of μ_{FET} versus T was found in a sample where the gate dielectric material was changed from SiO_2 to MgF_2 (24).

We conclude that grain boundaries, traps, and surface states (for charge densities $n > n_T$ and $T > T_T$) do not substantially influence the mobility in high-quality samples. We can thus extract values for J , γ , and

ω_0 that predict room-temperature mobilities for α -6T of $\sim 0.02 \text{ cm}^2 \text{ V}^{-1} \text{ s}^{-1}$, which is consistent with our highest measured room-temperature mobility (without high electric field effects), which is 0.02 to $0.03 \text{ cm}^2 \text{ V}^{-1} \text{ s}^{-1}$ (25). This result suggests that our TFTs already exhibit μ_{FET} close to the highest achievable μ_{FET} at 300 K , according to Holstein's formalism. Because, within this picture, the hopping mobility μ is proportional to $\exp(-E_B)$ (7), we can enhance μ by choosing materials with lower polaron binding energy or low carrier-lattice coupling.

REFERENCES AND NOTES

1. F. Garnier, R. Hajlaoui, A. Yassar, P. Srivastava, *Science* **265**, 1684 (1994).
2. A. Dodabalapur, L. Torsi, H. E. Katz, *ibid.* **268**, 270 (1995).
3. A. Dodabalapur, H. E. Katz, L. Torsi, R. C. Haddon, *ibid.* **269**, 1560 (1995).
4. A. J. Lovinger *et al.*, *J. Mater. Res.* **10**, 2958 (1995).
5. G. Horowitz, R. Hajlaoui, P. Delannoy, *J. Phys. III Fr.* **5**, 355 (1995); K. Wargai *et al.*, *Phys. Rev. B* **52**, 1786 (1995).
6. J. Ostrick *et al.*, unpublished results.
7. T. Holstein, *Ann. Phys.* **8**, 343 (1959).
8. N. F. Mott, *Metal-Insulator Transitions* (Taylor and Francis, London, 1990), pp. 59–68.
9. R. F. Kiehl *et al.*, *Phys. Rev. Lett.* **62**, 792 (1989).
10. L. Torsi, A. Dodabalapur, H. E. Katz, *J. Appl. Phys.* **78**, 1088 (1995).
11. H. E. Katz, A. Dodabalapur, L. Torsi, D. Elder, *Chem. Mater.* **7**, 2238 (1995).
12. S. M. Sze, *Physics of Semiconductor Devices* (Wiley, New York, 1981).
13. S. Kojima, *Phys. Rev. B* **47**, 2924 (1993).
14. E. M. Conwell, H. Y. Choi, S. Jayadev, *J. Phys. Chem.* **96**, 2827 (1992).
15. Along the transport direction, α -6T has a herringbone-type molecular arrangement. The crystal structure is described in (4) and in T. Siegrist *et al.*, *J. Mater. Res.* **10**, 2173 (1995). We take for the intermolecular spacing the nearest distance between adjacent molecules, which is $\sim 3.8 \text{ \AA}$.
16. M. G. Harrison, R. H. Friend, F. Garnier, A. Yassar, *Synth. Metals* **67**, 215 (1994).
17. I. G. Austin, *J. Phys. C* **5**, 1687 (1972).
18. Yu. A. Firsov, *Semiconductors* **29**, 515 (1995).
19. Some early batches of α -6T were dominated by extrinsic effects, and therefore the mobility at $T < T_T$ was too low to permit an observer to see the transition.
20. A. L. Shluger and A. M. Stoneham, *J. Phys. Condens. Matter.* **5**, 3049 (1993).
21. J. M. G. Cowie, *Polymers: Chemistry and Physics of Modern Materials* (Chapman and Hall, New York, 1991), pp. 256–257; S. Matsuoka, *Relaxation Phenomena in Polymers* (Hanser, New York, 1992), p. 224.
22. W. Warta and N. Karl, *Phys. Rev. B* **A32**, 1172 (1985).
23. L. Torsi *et al.*, *Chem. Mater.* **7**, 2247 (1995).
24. The transistors that have a MgF_2 gate dielectric also show all the features that transistors with a SiO_2 gate do.
25. It may be possible (but unlikely) that we are consistently underestimating μ_{FET} as a result of imperfect ohmic contacts. If this is the case, the data points and the calculated mobilities in Fig. 2 will be offset along the y axis.
26. We thank F. Capasso, E. A. Chandross, R. C. Haddon, P. B. Littlewood, A. J. Lovinger, A. P. Mills, J. C. Phillips, E. Reichmanis, G. Scamarcio, T. Siegrist, and R. E. Slusher for their encouragement and illuminating discussions.

30 January 1996; accepted 3 April 1996

Lithospheric Contributions to Arc Magmatism: Isotope Variations Along Strike in Volcanoes of Honshu, Japan

Annie B. Kersting,* Richard J. Arculus, David A. Gust

Major chemical exchange between the crust and mantle occurs in subduction zone environments, profoundly affecting the chemical evolution of Earth. The relative contributions of the subducting slab, mantle wedge, and arc lithosphere to the generation of island arc magmas, and ultimately new continental crust, are controversial. Isotopic data for lavas from a transect of volcanoes in a single arc segment of northern Honshu, Japan, have distinct variations coincident with changes in crustal lithology. These data imply that the relatively thin crustal lithosphere is an active geochemical filter for all traversing magmas and is responsible for significant modification of primary mantle melts.

Unraveling the extent to which arc magmas are modified during ascent is a prerequisite for understanding the primary petrologic characteristics of their sources and the petrogenetic

processes involved in magma generation. Isotopic data in combination with the chemical composition of arc lavas are crucial for tracing potential source contributions to these magmas (1). The major magma source in island arcs is the peridotitic mantle wedge, fluxed by subducted, slab-derived fluids (2). An additional contribution may come during magma passage through overriding lithosphere. For example, in the southern Andes, geochemical differences in andesite-rhyolite suites reflect increased crustal contributions to magma genesis coincident with an approximate doubling in crustal thickness to $>70 \text{ km}$ (3). Other

A. B. Kersting, Earth Science Division and Institute of Geophysics and Planetary Physics, Lawrence Livermore National Laboratory, L-231, Post Office Box 808, Livermore, CA 94551, USA.

R. J. Arculus, Key Centre for the Geochemical Evolution and Metallogeny of Continents, Department of Geology, Australian National University, Canberra, ACT 0200, Australia.

D. A. Gust, School of Geology, Queensland University of Technology, Brisbane, QLD 4001, Australia.

*To whom correspondence should be addressed.

LINKED CITATIONS

- Page 1 of 1 -



You have printed the following article:

Intrinsic Transport Properties and Performance Limits of Organic Field- Effect Transistors

L. Torsi; A. Dodabalapur; L. J. Rothberg; A. W. P. Fung; H. E. Katz

Science, New Series, Vol. 272, No. 5267. (Jun. 7, 1996), pp. 1462-1464.

Stable URL:

<http://links.jstor.org/sici?sici=0036-8075%2819960607%293%3A272%3A5267%3C1462%3AITPAPL%3E2.0.CO%3B2-W>

This article references the following linked citations. If you are trying to access articles from an off-campus location, you may be required to first logon via your library web site to access JSTOR. Please visit your library's website or contact a librarian to learn about options for remote access to JSTOR.

References and Notes

¹ **All-Polymer Field-Effect Transistor Realized by Printing Techniques**

Francis Garnier; Ryad Hajlaoui; Abderrahim Yassar; Pratima Srivastava

Science, New Series, Vol. 265, No. 5179. (Sep. 16, 1994), pp. 1684-1686.

Stable URL:

<http://links.jstor.org/sici?sici=0036-8075%2819940916%293%3A265%3A5179%3C1684%3AAFTTRBP%3E2.0.CO%3B2-C>

² **Organic Transistors: Two-Dimensional Transport and Improved Electrical Characteristics**

A. Dodabalapur; L. Torsi; H. E. Katz

Science, New Series, Vol. 268, No. 5208. (Apr. 14, 1995), pp. 270-271.

Stable URL:

<http://links.jstor.org/sici?sici=0036-8075%2819950414%293%3A268%3A5208%3C270%3AOTTTAI%3E2.0.CO%3B2-E>

³ **Organic Heterostructure Field-Effect Transistors**

A. Dodabalapur; H. E. Katz; L. Torsi; R. C. Haddon

Science, New Series, Vol. 269, No. 5230. (Sep. 15, 1995), pp. 1560-1562.

Stable URL:

<http://links.jstor.org/sici?sici=0036-8075%2819950915%293%3A269%3A5230%3C1560%3AOHFT%3E2.0.CO%3B2-A>

NOTE: *The reference numbering from the original has been maintained in this citation list.*